



**HAL**  
open science

## Synthesis of boron carbide from its elements up to 13 GPa

Amrita Chakraborti, Nicolas Guignot, Nathalie Vast, Yann Le Godec

► **To cite this version:**

Amrita Chakraborti, Nicolas Guignot, Nathalie Vast, Yann Le Godec. Synthesis of boron carbide from its elements up to 13 GPa. *Journal of Physics and Chemistry of Solids*, 2021, 159, pp.110253. 10.1016/j.jpcs.2021.110253 . hal-03411852

**HAL Id: hal-03411852**

**<https://hal.science/hal-03411852v1>**

Submitted on 2 Nov 2021

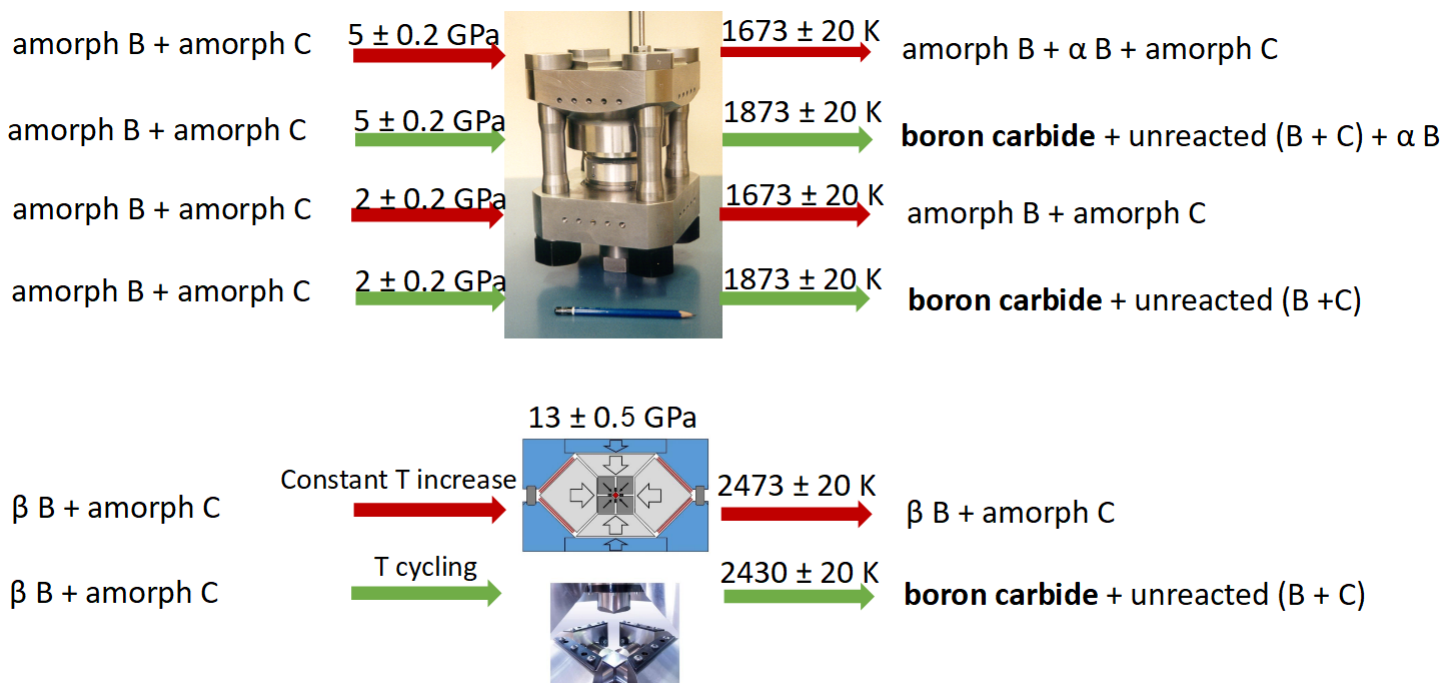
**HAL** is a multi-disciplinary open access archive for the deposit and dissemination of scientific research documents, whether they are published or not. The documents may come from teaching and research institutions in France or abroad, or from public or private research centers.

L'archive ouverte pluridisciplinaire **HAL**, est destinée au dépôt et à la diffusion de documents scientifiques de niveau recherche, publiés ou non, émanant des établissements d'enseignement et de recherche français ou étrangers, des laboratoires publics ou privés.

# Graphical Abstract

## Synthesis of boron carbide from its elements up to 13 GPa

Amrita Chakraborti, Nicolas Guignot, Nathalie Vast, Yann Le Godec



## Highlights

### **Synthesis of boron carbide from its elements up to 13 GPa**

Amrita Chakraborti, Nicolas Guignot, Nathalie Vast, Yann Le Godec

- Optimal temperature and reactants parameters for boron carbide at unprecedented high pressure values
- Pressure influences carbon content of boron carbide formed
- Temperature cycling appears to reduce temperature of formation of boron carbide as compared to constant heating

# Synthesis of boron carbide from its elements up to 13 GPa

Amrita Chakraborti<sup>a</sup>, Nicolas Guignot<sup>b</sup>, Nathalie Vast<sup>a</sup>, Yann Le Godec<sup>c</sup>

<sup>a</sup>*Laboratoire des Solides Irradiés, CEA/DRF/IRAMIS, CNRS UMR 7642, École Polytechnique, Institut Polytechnique de Paris, 28 Route de Saclay, F-91120, Palaiseau, France*

<sup>b</sup>*Synchrotron SOLEIL, Gif-sur-Yvette, France*

<sup>c</sup>*Institut de Minéralogie, de Physique des Matériaux et de Cosmochimie (IMPMC), Sorbonne Université, UMR CNRS 7590, Muséum National d'Histoire Naturelle, IRD UMR 206, 4 Place Jussieu, 75005, Paris, France*

---

## Abstract

The synthesis of boron carbide from its elements (boron and carbon) has been studied under pressures up to 13 GPa and optimum parameters have been determined by varying the (P, T, reactants) conditions. Stoichiometric mixtures of amorphous boron and amorphous carbon have been subjected to a range of temperatures from 1673 K to 2273 K at the pressure values of 2 GPa and 5 GPa. The formation temperatures have been compared to those obtained from mixtures of  $\beta$  rhombohedral boron and graphite, and  $\beta$  rhombohedral boron and amorphous carbon at 2 GPa and 5 GPa. The formation temperature is thus shown to be affected by the pressure and the choice of the reactants. The carbon concentration of boron carbide is also shown to be affected by pressure at which it is synthesised from elements, and we propose pressure as a means to control the carbon content. Temperature cycling has also been shown to reduce the formation temperature of boron carbide at 13 GPa. The formation of  $\alpha$  rhombohedral boron as an intermediate phase is seen at 5 GPa before the formation of boron carbide.

### *Keywords:*

HPHT synthesis, boron carbide, pressure effects, Paris-Edinburgh press, multi-anvil cell

---

## 1. Introduction

Boron carbide is an important ceramic with wide ranging applications such as abrasives, safety armours and bullet-proof jackets (1). These applications originate in its remarkable properties such as high hardness (2) - the Vickers hardness is 38 GPa, a specific density as low as 2.52 g/cc (3), and high chemical stability (1; 4; 5).

Industrial production of boron carbide occurs through carbothermic or magnesiothermic reactions (3; 6; 7), since these processes are the most feasible in an economic context. However, boron carbide synthesised through these processes have considerable impurity content. An alternative is to produce boron carbide from elements - very pure boron and carbon - this results in the production of highly pure boron carbide (6). Thus, the synthesis of boron carbide from its elements is particularly important when the purity of the final product is a priority.

A number of studies have been done on the synthesis of boron carbide from different reactants at ambient pressure or at low pressures (<50 MPa) (5; 8). There have also been quite a few studies on the properties of boron carbide crystals when subjected to high pressures (9; 10; 11; 12; 13). One study has reported the synthesis of single crystal boron carbide without disorder at 8 GPa, but the reactants used for the synthesis were not mentioned (14). Boron carbide single crystal nanoparticles have also been synthesised in vacuum (15) and single crystalline boron carbide nanobelts have been synthesised using chemical vapour deposition (CVD) at atmospheric pressure (16).

Moreover, *ab initio* calculations have found evidence of new phases in boron carbide at HPHT conditions (17; 18). In order to provide experimental verification of these phases, we need to synthesise boron carbide in HPHT conditions. However, during this endeavour, we found that there was a lack of systemic study of boron carbide synthesis at high pressure in the literature. Thus, one of the motivations of the current study was to create such a toolbox for HPHT synthesis of boron carbide.

Some groups have investigated the B-C system at high pressures and temperatures (19; 20). However, this work, along with Ref. (21), is a first attempt to create a toolbox for the high pressure and temperature synthesis parameters of boron carbide from crystalline and amorphous phases of boron and carbon.

The previous work (21) was performed with limited (P, T, reactants)

conditions. The reactants were either  $\beta$  rhombohedral boron and amorphous carbon or  $\beta$  rhombohedral boron and graphite.

Consequently, a systematic study of the formation of boron carbide at high pressure up to 13 GPa has been performed in the current work in order to fix the optimum parameters for synthesis. The objective is to find out the optimal conditions of pressure, temperature and reactants to form boron carbide from its elements. The direct synthesis from the elements avoids the formation of ternary products, which simplifies the characterisation process (22).

In the present work, the optimum (P, T, reactants) parameters of the synthesis of boron carbide from elements (boron and carbon) have been analysed for 2 GPa and 5 GPa for three combination of reactants: a)  $\beta$  rhombohedral boron and amorphous carbon, b)  $\beta$  rhombohedral boron and graphite and c) amorphous boron and amorphous carbon using the Paris-Edinburgh press. At 5 GPa, we find that an intermediate phase precedes the formation of boron carbide and thus competes with the formation of boron carbide - this is observed at 5 GPa, but not at 2 GPa. Moreover, the formation temperature at 13 GPa has been studied using, as reactant mixture,  $\beta$  rhombohedral boron and amorphous carbon using a different press with respect to Ref. (21): a multi-anvil cell. The syntheses have also been studied *in situ* at the SOLEIL Synchrotron for the first time.

In Sec. 2, the materials and methods used in the current work are presented. We report our results in Sec. 3, and this is followed by discussions in the next section. Conclusions are drawn in Sec. 5.

## 2. Materials and methods

### 2.1. Synthesis conditions at 2 and 5 GPa

The methodology of the synthesis experiments done in the Paris-Edinburgh press at 2 and 5 GPa has been discussed in an earlier work (21). Additional experiments have been performed in the current work at 2 GPa and 5 GPa using the same methodology starting with a reactant mixture of amorphous boron (Pavezyum, purity >98.5 %, particle size <250nm) and glassy amorphous carbon (Sigma-Aldrich, purity 99.95 % trace metals basis, particle size 2 – 20 microns). The sample volume produced at each run was around 50 mm<sup>3</sup>.

The pressure values have been chosen because of the following reasons: 5 GPa is the maximum pressure that can be attained in the Paris-Edinburgh

press with a 10 mm gasket that would provide enough sample after recovery for *in situ* characterisation. 2 GPa is on the lower limit of the pressure that can be attained in the press with high temperatures.

Some *in situ* experiments were also performed in the PSICHE beamline of the SOLEIL synchrotron. The *in situ* experiments not only help us to confirm the results obtained from *in situ* syntheses but are also critical for understanding the mechanism of the synthesis, especially when the intermediate phase forms. This is the first time *in situ* synthesis of boron carbide from elements has been done, since the low atomic number of boron and carbon and hence the lower X-ray scattering by these elements poses a challenge.

For these *in situ* experiments, the samples were subjected to the desired pressure and then the temperature was slowly increased. At each step of the temperature increase, a diffractogram of the sample centre was produced using the white synchrotron beam in order to understand the evolution of the reactants into the final product in real time. The white beam has an energy range of 15 - 80 keV and it is focused to a size of 25  $\mu\text{m}$  (in the vertical direction) on the sample, collimated to 50  $\mu\text{m}$  in the horizontal direction. The diffractograms were taken at various sample positions in order to ensure the homogeneity of the reactions.

Energy dispersive X-ray diffraction (EDXRD) is the usual configuration used for large volume press (LVP) experiments in the PSICHE beamline. The EDXRD is complemented by the CAESAR system. The PSICHE beamline in SOLEIL synchrotron is the only one in Europe to provide the CAESAR facility, originally proposed by Wang *et al.* (23). Whereas EDXRD is advantageous for large volume press experiments in synchrotron environments because of its rapid acquisition time, background and waste signal removing efficiency, and high efficiency in working with limited sample volume and aperture, it has numerous disadvantages as well. The most important among these disadvantages are the complex corrections for intensity required for the Rietveld refinement and the presence of detector artifacts. One-dimensional (1D) *in situ* ADXRD techniques can be used to overcome these shortcomings, but they require a special Soller slits system to remove the signal from the sample environment [88]. Thus, the combination of the complementary ADXRD and EDXRD in one system, as done in CAESAR, overcomes their respective drawbacks. The CAESAR system provides access to a higher  $Q$  range and peaks intensities are well resolved which makes the data collected suitable for structural refinement.

For all EDXRD as well as CAESAR measurements, rotating Ge solid-

state detector is used. Three collimating slits are also present: one is positioned in front of the press and the other two are positioned between the press and the detector.

The EDXRD diffractograms were each taken for 2 minutes each. The data obtained with the synchrotron radiation has been converted to Cu K $\alpha$  in order to facilitate the treatment and analysis of the data and to compare these *in situ* data to the *ex situ* results.

## 2.2. Synthesis conditions at 13 GPa

Two syntheses at 13 GPa were also performed using a mixture of crystalline  $\beta$  boron (Prolabo, purity 99.9% , particle size 1-10 microns) and glassy amorphous carbon which have been mixed in a special cBN mortar and pestle for 5 minutes in the stoichiometric ratio of 4:1. Both the *in situ* and *ex situ* experiments were performed using the DIA module of the multi-anvil press (24; 25). A pressure of  $13\pm 0.5$  GPa was attained in both cases over a span of 8 hours.

The pressure value of 13 GPa was chosen as it is the maximum pressure that we could attain in the multi-anvil press *in situ* at very high temperatures with a functioning thermocouple.

### 2.2.1. Application of $(P, T)$ conditions in the *in situ* experiments at 13 GPa

The *in situ* experiment was performed in the PSICHE beamline of the SOLEIL synchrotron.

For the *in situ* experiment, the reactant mixture was put in the set-up (set-up 1) shown in figure 1. Pressure was estimated using MgO as a pressure calibrant (26; 27). The sample volume produced using this set-up was around  $13 \text{ mm}^3$ .

Some studies in the literature have suggested that thermal cycling can effect the rate of chemical reactions (28; 29; 30). However, it is difficult to study the effects of thermal cycling in high pressure experiments because the cycling temperature might cause a blowout of the pressure cell. That is why we designed a thermal cycling experiment to be done *in situ* as SOLEIL synchrotron where we could monitor the sample in real time and watch out carefully for changes in the sample at each cycle as well as monitor any blowout of the cell.

Therefore, the temperature for the *in situ* experiment was not increased uniformly (*i.e.* at a constant rate) to the final dwell temperature, as was done in the case of the other experiments. Instead, a thermal cycling was applied

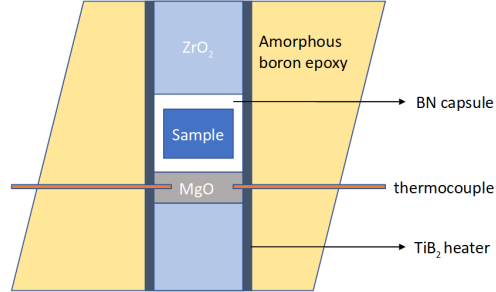


Figure 1: Set-up 1: The sample assembly used for the *in situ* multi-anvil experiment.  $\text{TiB}_2$  heater was used inside an amorphous boron epoxy octahedron. The sample capsule is made of hexagonal boron nitride (hBN).

in order to observe its effects. The temperature route has been described in table 1. The temperature of the sample was increased to a specific value for around 3 minutes, the EDXRD pattern was recorded in the center of the sample, and the temperature was then dropped to 300 K. Next, the temperature of the same sample was again raised to the next higher value and the same process was repeated. The upper limit of the temperature that was attained in each successive cycle has been recorded in table 1. After the final quenching to 300 K, the sample was decompressed slowly over 4 hours. Finally, a diffractogram was taken using the CAESAR system.

Cycle number	Lower temperature	Higher temperature	Phases found in EDXRD
1	300 K	875 K	$\beta$ boron
2	300 K	1170 K	$\beta$ boron
3	300 K	1360 K	$\beta$ boron
4	300 K	1670 K	$\beta$ boron
5	300 K	1912 K	$\beta$ boron
6	300 K	2430 K	boron carbide

Table 1: The upper and lower values of temperature attained during each cycle of the same sample in the *in situ* run, along with the phases found *in situ* in each cycle at the higher temperature using EDXRD.

### 2.2.2. Application of $(P, T)$ conditions in the *ex situ* experiments at 13 GPa

For the *ex situ* experiment, a different type of set up was used (set-up 2), as shown in figure 2. The main differences are the use of rhenium foil as the

heater and  $\text{LaCrO}_3$  sleeve as a thermal insulator. The metal heater enables us to have a larger sample volume compared to set-up 1, which is important for subsequent *ex situ* characterisation. The temperature was raised slowly and constantly at a rate of 2 K/s to a final value of 2473 K. Temperature was measured using a type C thermocouple (W 5 % Re/ W 26 % Re) with an error of evaluation of  $\pm 20$  K. Then, the sample was subjected to a dwell time of 30 minutes to the *ex situ* sample: no thermal cycling was performed on this sample.

Pressure was fixed at 13 GPa by using a calibration curve determined through previous *in situ* calibrations in synchrotron SOLEIL, with an error of evaluation of  $\pm 0.2$  GPa (31). The sample volume produced using this set-up was around  $20 \text{ mm}^3$ .

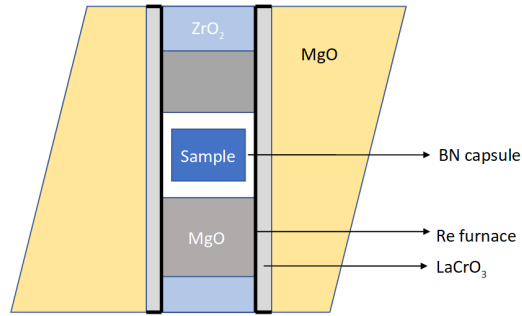


Figure 2: Set-up 2: The sample assembly used for the *ex situ* multi-anvil experiment. Rhenium foil was used as a heater instead of the  $\text{LaCrO}_3$  used in the *in situ* run.

After the dwell time of 30 minutes, the sample was quenched rapidly by removing the electrical power. The decompression was done slowly over the span of 4 hours. The sample was then recovered carefully and subjected to characterisation by *ex situ* X-ray diffraction.

### 3. Results

#### 3.1. *Ex situ* and *in situ* diffraction at 2 and 5 GPa

We define the formation temperature as the lowest temperature where we observe the formation of boron carbide. The optimal temperature, on the other hand, is defined as the lowest observed temperature at which boron carbide is the prominent product.

Further syntheses performed in this work has confirmed the preliminary results of our previous work (21) to find out the formation temperatures and optimal temperatures of boron carbide at 2 and 5 GPa using reactant mixtures of a)  $\beta$  boron and amorphous carbon, and b)  $\beta$  boron and graphite. Moreover, in the current work, we have further expanded the scope of the study by using other reactants (amorphous boron), higher pressure values, temperature cycling as well as *in situ* syntheses. The results have been tabulated in table 2. Also, the intermediate phase ( $\delta$ ) observed during the syntheses under 5 GPa from  $\beta$  boron and amorphous carbon has been identified as  $\alpha$  rhombohedral boron.

In the current work, the mixture of amorphous boron and amorphous carbon have been subjected to a pressure of  $2 \pm 0.2$  GPa and  $5 \pm 0.2$  GPa respectively. At 2 GPa, the formation temperature of boron carbide is  $1873 \pm 20$  K. In figure 3, we report the XRD pattern showing the synthesis of boron carbide from amorphous boron and amorphous carbon at 2 GPa. The signal to background ratio might vary a little from sample to sample because of the slight differences in the amount of the sample recovered for *ex situ* characterisations after each run.

At 5 GPa as well, the temperature of formation of boron carbide decreases from  $2273 \pm 20$  K (when  $\beta$  boron is used as a reactant) to  $1873 \pm 20$  K. In figure 4, the XRD patterns at various temperatures for the 5 GPa series are shown. It is observed that only very small XRD peaks of boron carbide appear at temperatures of synthesis of 1873 K and 2073 K. At these temperatures (1873 K and 2073 K), an intermediate phase, that we have identified as  $\alpha$  rhombohedral boron remained the most prominent phase. Boron carbide becomes the most prominent phase at 2273 K, similar to what was observed during the syntheses with  $\beta$  boron and amorphous carbon (21).

Moreover, similar to the case of synthesis from  $\beta$  boron and amorphous carbon in Ref. (21), no formation of  $\alpha$  boron was recorded for the syntheses with amorphous boron at 2 GPa.

Additionally, *in situ* synthesis at 2 GPa, in figure 5, with a reactant mixture of  $\beta$  boron and amorphous carbon, corroborated the *ex situ* results reported in Ref. (21) - boron carbide forms at 2073 K from a mixture of  $\beta$  boron and amorphous carbon under a pressure of 2 GPa. The diffractograms were taken within 5 minutes of raising the temperature each time, unlike the 2 hour dwell time that the samples were subjected to for the *ex situ* syntheses. This means that the reactions were still incomplete when the diffractograms were taken - this is the reason behind the presence of  $\beta$  boron and amorphous

carbon in the diffractograms even at high temperatures.

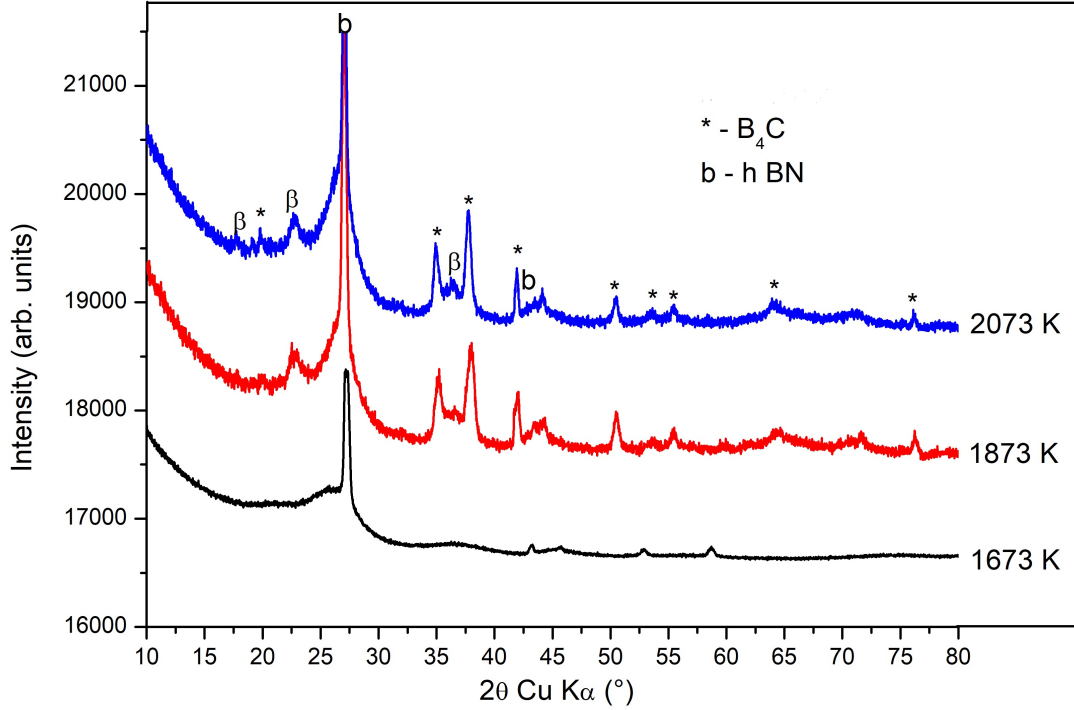


Figure 3: *Ex situ* X-ray diffraction pattern of quenched sample from the mixture of amorphous boron and amorphous carbon under 2 GPa for 2 hours. It is shown that boron carbide (32) is formed at 1873 K with the amorphous boron reactant. No  $\alpha$  boron is formed. The hBN peaks come from the capsule enclosing the sample, and not from the sample itself.

### 3.2. Diffraction at 13 GPa

We also report the results at 13 GPa.

During the *in situ* run at 13 GPa, a series of EDXRD patterns were taken immediately after the temperature was raised in each cycle and before the system was quenched. Figure 6 shows the EDXRD patterns as a function of rising temperature at 13 GPa. In the figure, the data obtained with the synchrotron radiation has been converted to Cu  $K\alpha$  in order to facilitate the treatment and analysis of the data.

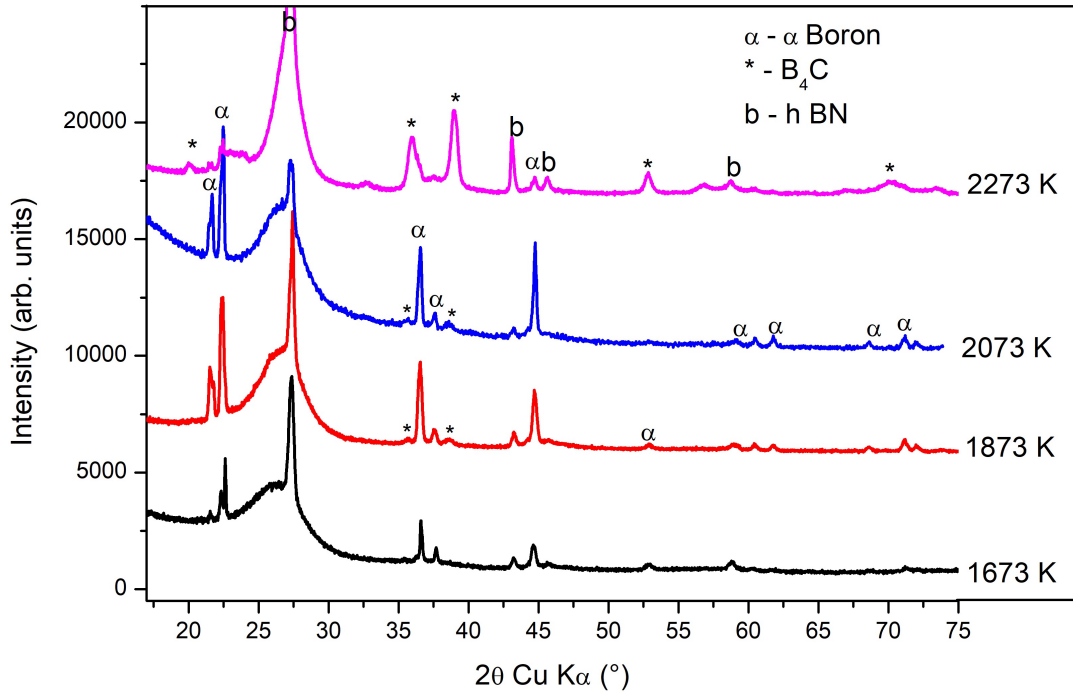


Figure 4: *Ex situ* X-ray diffraction pattern of quenched sample from the mixture of amorphous boron and amorphous carbon under 5 GPa for 2 hours. It is shown that boron carbide (32) starts forming at 1873 K with the amorphous boron reactant, with  $\alpha$  boron remaining the prominent phase. Boron carbide becomes the prominent phase at 2273 K. The hBN peaks come from the capsule enclosing the sample, and not from the sample itself.

As the upper limit of temperature is increased in each cycle, only some  $\beta$  boron peaks are observed up to 1912 K. Some peaks of  $\beta$  boron are different from one cycle to another: this can be attributed to the recrystallisation of  $\beta$  boron under high pressure and temperature conditions (35).

However, in the last cycle, as temperature is increased to 2430 K, most of the  $\beta$  boron has reacted and the formation of boron carbide is observed.

After the last cycle of temperature increase, the system is quenched and EDXRD is performed again to observe whether boron carbide remains in the system. As the final EDXRD pattern in figure 6 shows, the boron carbide peaks have remained unchanged after quenching.

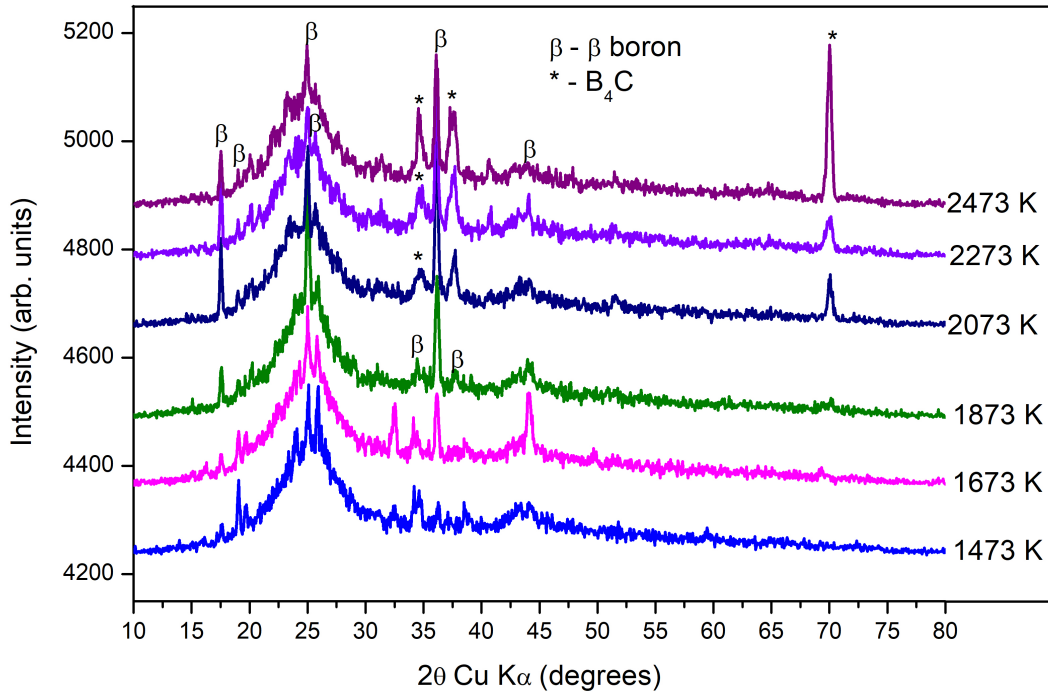


Figure 5: *In situ* diffraction pattern taken at the center of the sample of a mixture of crystalline boron and amorphous carbon at 2 GPa. The data obtained from the synchrotron radiation was converted to that of Cu  $K\alpha$  radiation.

After this, the sample was decompressed and another XRD pattern was taken using the CAESAR system. The CAESAR pattern in figure 7 also shows the presence of boron carbide in the recovered sample.

In order to verify whether the temperature cycling had any effect on the formation of boron carbide, a second experiment was performed. In this *ex situ* experiment, the temperature was raised to 2473 K slowly without any cycling. The XRD performed on the recovered sample after the experiment is shown in figure 8: no boron carbide peaks have been observed in the sample. In order to establish this observation, the XRD diffractogram has been compared to that of boron carbide formed at 2473 K under 2 GPa in the inset of figure 8. The  $2\theta$  angle domain between  $33^\circ$  -  $40^\circ$  (in inset of figure 8) shows the most prominent peaks of boron carbide (012) and (104) under

Reference	Pressure (GPa)	Reactants	heating rate	Formation temp. (K)	Optimal temp. (K)
Wang <i>et al.</i> , 2009 (33)	0.02	B + graphite	constant	1573	-
Roszeitis <i>et al.</i> , 2014 (34)	0.05	B + graphite	constant	1606	-
This work	$2 \pm 0.2$	amorph. B + amorph. C	constant	$1873 \pm 20$	1873
This work	$5 \pm 0.2$	amorph. B + amorph. C	constant	$1873 \pm 20$	2273
Our work, 2020 (21)	$2 \pm 0.2$	$\beta$ B + amorph. C	constant	$2073 \pm 20$	2073
Our work, 2020 (21)	$2 \pm 0.2$	$\beta$ B + graphite	constant	$2273 \pm 20$	>2273
Our work, 2020 (21)	$5 \pm 0.2$	$\beta$ B + amorph. C	constant	$2273 \pm 20$	2273
Our work, 2020 (21)	$5 \pm 0.2$	$\beta$ B + graphite	constant	$2473 \pm 20$	>2573
This work	$13 \pm 0.5$	$\beta$ B + amorph. C	cycling	$2430 \pm 20$	>2430
This work	$13 \pm 0.2$	$\beta$ B + amorph. C	constant	>2473	>2473

Table 2: Summary of the formation temperatures and optimal temperatures of formation of boron carbide from elemental boron and carbon, depending on the pressure and on the solid-state form of carbon and boron, in ascending order of formation temperature and pressure.

Cu K $\alpha$  radiation. As is evident from the comparison, the sample quenched after a HPHT treatment at 13 GPa and 2473 K does not contain any boron carbide. Some trace amounts of  $\gamma$  orthorhombic boron (37) was found in the sample, but no  $\alpha$  boron was formed, contrary to the case at 5 GPa. At 13 GPa, after heating to 2473 K, the quenched sample is overwhelmingly composed of  $\beta$  rhombohedral boron.

### 3.3. Raman spectroscopy at 13 GPa

Figure 9 shows the results of the Raman spectroscopy done on the recovered samples from the *in situ* and *ex situ* syntheses. Crystalline  $\beta$  boron peaks were found in both samples, while the *in situ* synthesis had additional boron carbide peaks. No peaks corresponding to  $\gamma$  boron or  $\alpha$  boron were found in either of the samples.

## 4. Discussions

### 4.1. Search for the optimal synthesis parameters

The synthesis at 2 GPa follows a well-understood and direct path, similar to what has been reported in the literature (33; 34) for the low pressure

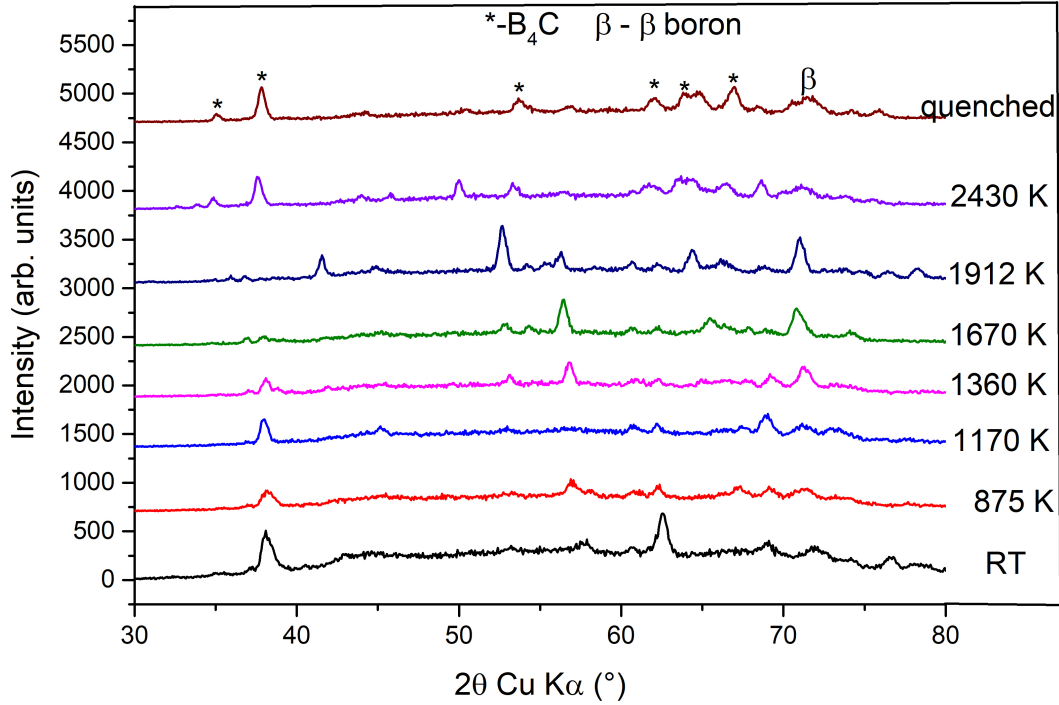


Figure 6: Temperature cycling at 13 GPa: *In situ* diffraction pattern taken at the center of the sample of a mixture of crystalline  $\beta$  boron and amorphous carbon at 13 GPa for various temperatures during the *in situ* run. The data obtained from the synchrotron radiation was converted to that of Cu K $\alpha$  radiation. All the unmarked peaks are those of crystalline  $\beta$  boron. No peaks were visible in the  $20^\circ$ -  $30^\circ$  interval, and hence, this range has been omitted from the figure

syntheses. However, the formation temperature increases considerably compared to the low pressure syntheses. A temperature increase by more than 250 K with respect to that of ambient pressure is required to form boron carbide at 2 GPa. Only by 1873 K (in the case of amorphous boron and amorphous carbon), 2073 K (in the case of  $\beta$  boron and amorphous carbon) and 2273 K (in the case of  $\beta$  boron and graphite) does boron carbide start forming.

Regarding the optimisation of the synthesis conditions, amorphous carbon turns out to be a better reactant than graphite for synthesising boron carbide at elevated pressures, since the use of graphite requires an even higher forma-

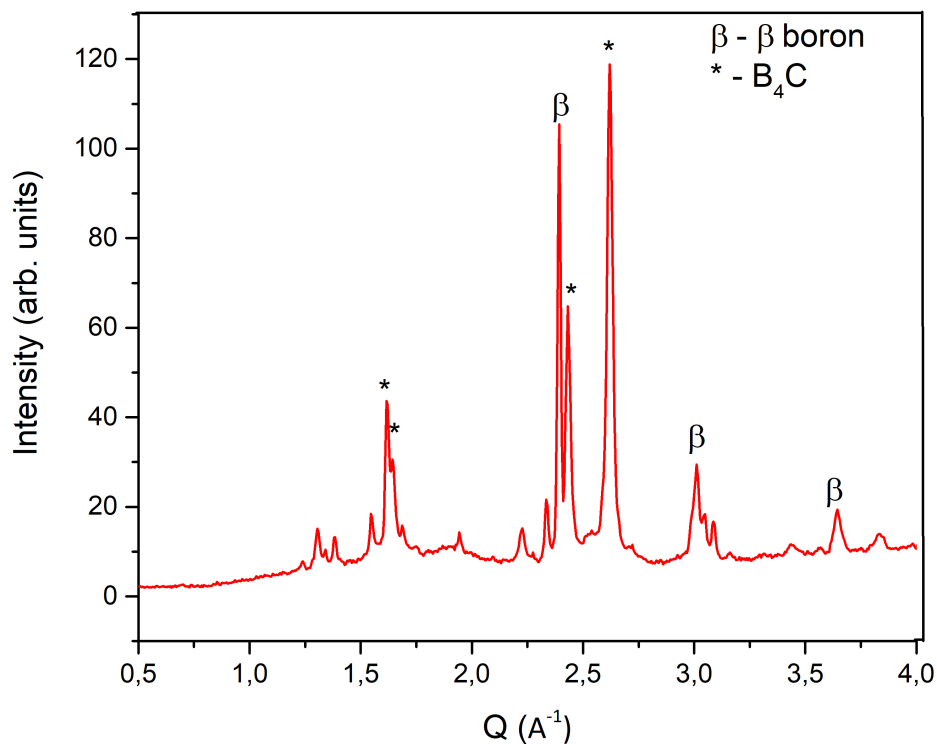


Figure 7: Temperature cycling at 13 GPa: *In situ* diffraction pattern taken at the center of the sample of a mixture of crystalline  $\beta$  boron and amorphous carbon at ambient conditions after applying a pressure of 13 GPa and temperature cycling during the *in situ* run. The data was obtained from the synchrotron radiation using the CAESAR system (36). All the unmarked peaks are those of crystalline  $\beta$  boron.

tion temperature. This is attributed to the higher reactivity of amorphous carbon because of its high concentration of dangling bonds (39; 40; 41). Also, carbon atoms have higher mobility in amorphous carbon than in graphite (42). The higher mobility of the carbon atoms increases the diffusion of carbon throughout the reacting mixture - this allows the reactants to come in contact with each other thus leading to synthesis of boron carbide at lower temperatures.

Amorphous boron is also found to be a better reactant than  $\beta$  boron - this can also be attributed to the better reactivity of amorphous boron compared

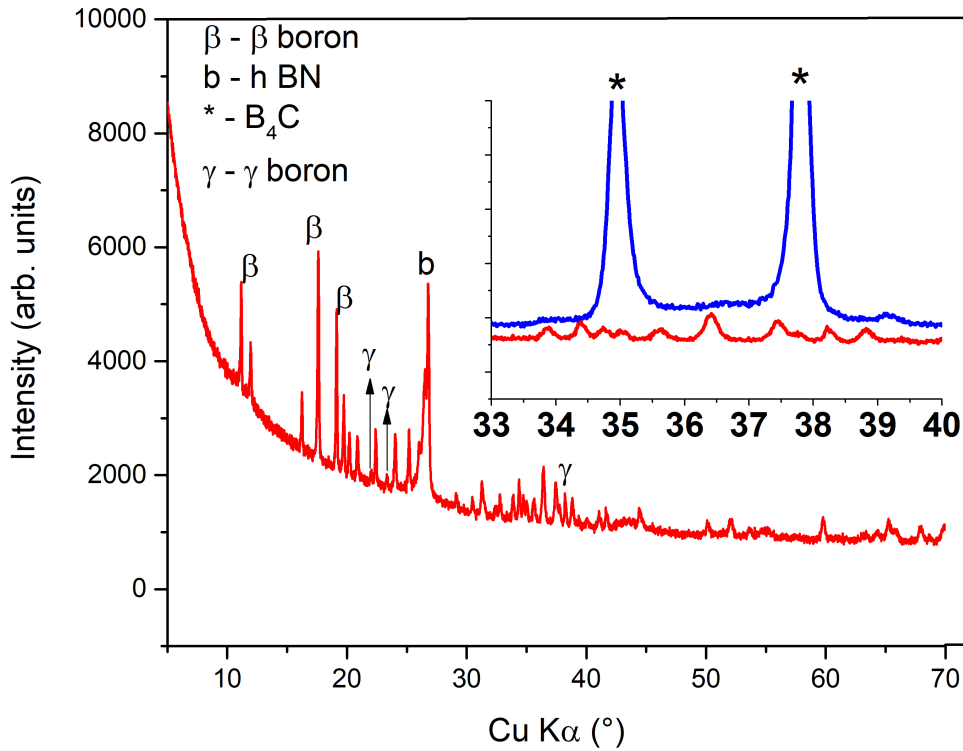


Figure 8: Constant heating rate at 13 GPa: X-ray diffraction pattern of quenched sample from the mixture of crystalline  $\beta$  boron (38) and amorphous carbon under 13 GPa at 2473 K for 1 hour. The inset is the zoom between 33 ° and 40 ° of the superposition of the curve of the product (same colour as main plot) and the diffractogram of conventional  $B_4C$ . It is shown that no new peaks corresponding to boron carbide (32) form in the sample. The hBN peaks come from the capsule enclosing the sample, and not the sample itself.

to crystalline boron due to the absence of an ordered crystalline structure (43; 44; 45).

Moreover, the higher reactivity of amorphous boron and carbon can also be attributed to the higher surface area available in amorphous substances leads to greater contact area for reactions to take place, compared to their crystalline counterparts.

At 5 GPa, the reaction with both amorphous boron and  $\beta$  boron pro-

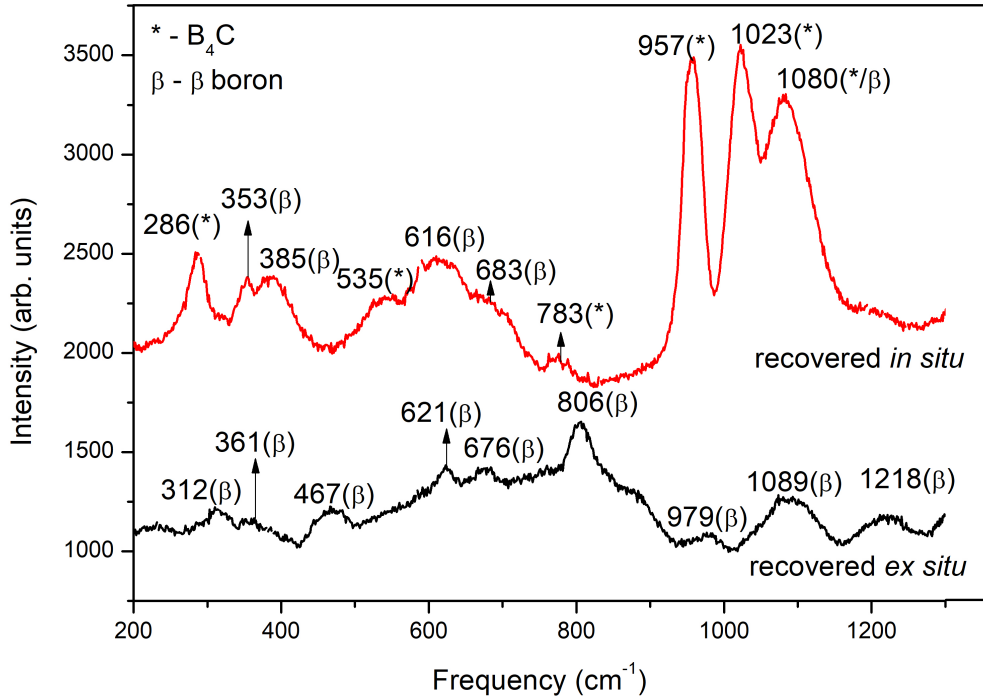


Figure 9: Raman spectroscopy of recovered samples from the *in situ* (temperature cycling) and *ex situ* (constant heating) synthesis at 13 GPa. The *ex situ* sample shows only  $\beta$  boron peaks after HPHT treatment, while the *in situ* sample shows both  $\beta$  boron and boron carbide peaks.

duce  $\alpha$  boron as the prominent product up to 2073 K. This indicates that  $\alpha$  boron is an intermediate step towards the formation of boron carbide from amorphous or  $\beta$  boron and amorphous carbon under a pressure of 5 GPa.

The formation temperature also increases with the increase of pressure in all of the cases except for that of amorphous boron as reactant. Yang *et al.* (44) have suggested that high pressure can decrease the reaction efficiency of boron greatly. In their experiments, the evaporation rate of the surface boron oxide would decrease as the pressure increased. However this does not explain the reason behind the increase of formation temperature when amorphous carbon is replaced by graphite, as the same crystalline  $\beta$  boron was used in both cases. Another possible explanation is that high pressure may

inhibit the diffusion of carbon atoms through the interstitial spaces in crystalline boron and thus, it would slow down the reaction. The application of higher temperature values would then favour the diffusion process that leads to the formation of boron carbide. In another study, it has also been noted that an inverse relationship between pressure and the reaction constant exists at the high pressure limit for chemically activated reactions (46). Therefore, as the pressure applied during the synthesis increases, the reaction rate falls. This effect can be compensated by an increase in temperature, which results in the increased formation temperature of boron carbide. Thus, temperature can be said to act as negative pressure (17), and so higher temperature at higher pressure may be the signature that the change in diffusion due to pressure is compensated by the change in diffusion due to temperature. This relationship between the rate of change of the diffusion constant with temperature and pressure in the case of formation of boron carbide from its elements under pressure has been expressed in equation 1.

$$\frac{\partial D}{\partial T} = -k \frac{\partial D}{\partial P} \quad (1)$$

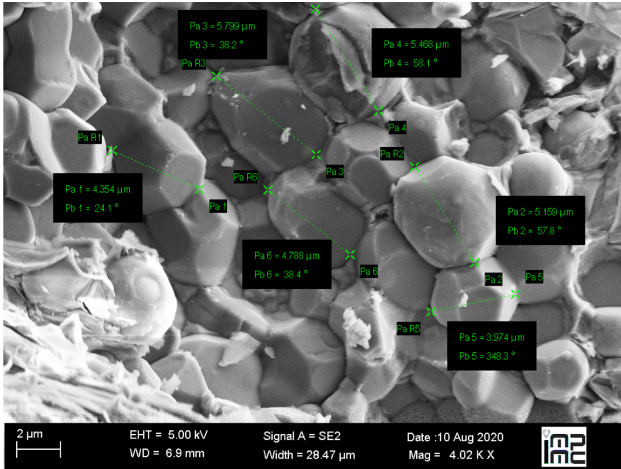
where D is the diffusion constant of carbon or boron atoms, T is the temperature, P is the pressure and k is the constant of proportionality.

#### *4.2. Crystallite size and particle size*

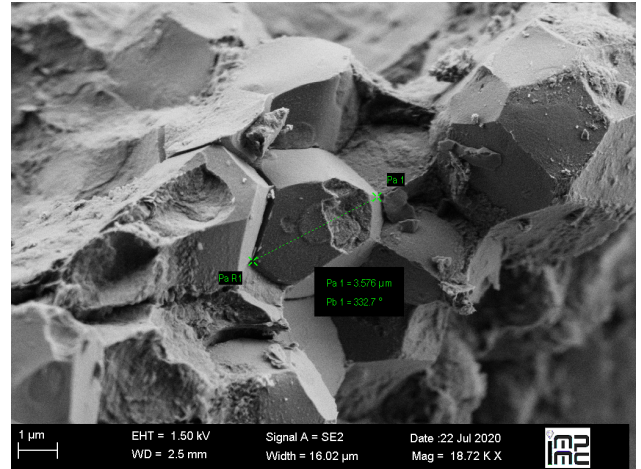
The crystallite size in this section refers to the coherently scattering domain size: the Scherrer formula is only applicable for this domain. This is different from the particle size as the particle size can be thought of as the agglomerate of many crystallites. Therefore, the crystallite size would then be the lower bound of particle size. The lower bound of the average crystallite size of the boron carbide as synthesised at 2 and 5 GPa has been determined using the Scherrer formula (47). The average crystallite size (about 25 nm) was found to decrease with pressure, and to increase with the formation temperature. The size was also found to slightly decrease when graphite is used as a reactant instead of amorphous carbon. Concerning the granulometry of the powder, scanning electron microscopy showed a particle size of 3 - 6 microns irrespective of reactant mixture or formation temperature, as shown in figure 10.

#### *4.3. Carbon content of the synthesised boron carbide*

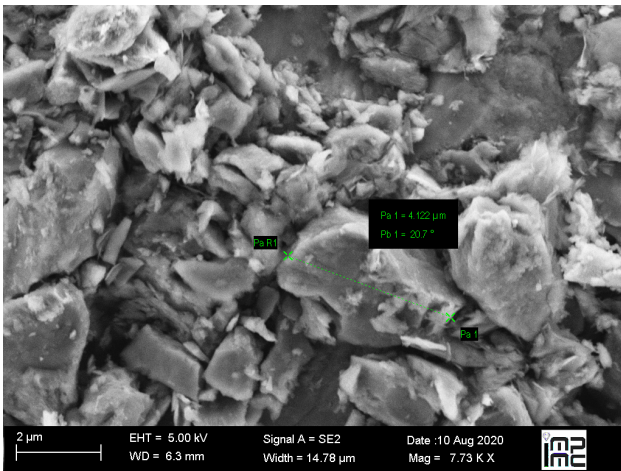
It is also worthwhile to try to find out the carbon concentration of the boron carbide synthesised using different reactants and different pressures. It



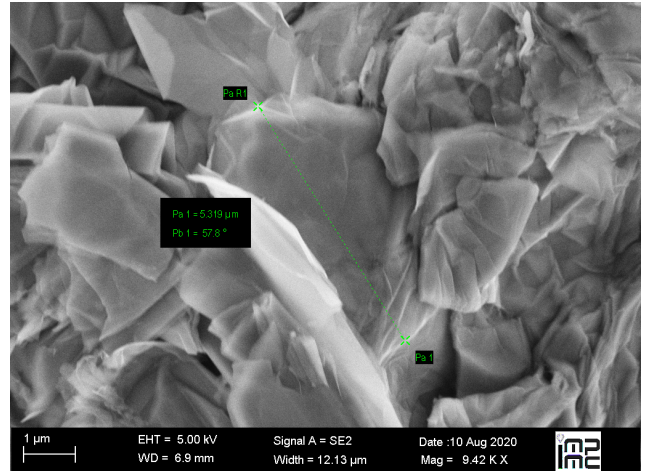
(a) beta B + amorph C, 2 GPa, 2073 K



(b) beta B + amorph C, 5 GPa, 2473 K



(c) amorph B + amorph C, 5 GPa, 2473 K



(d) beta B + graphite, 2 GPa, 2473 K

Figure 10: Some selected Scanning electron microscopy images at ambient conditions of the recovered boron carbide formed after being treated at (a) 2 GPa, 2073 K for  $\beta$  boron and amorphous carbon, (b) 5 GPa, 2473 K for  $\beta$  boron and amorphous carbon, (c) 5 GPa, 2473 K for amorphous boron and amorphous carbon and (d) 2 GPa, 2473 K for  $\beta$  boron and graphite. The image (a) shows particle sizes of 3.5  $\mu\text{m}$  to 5.7  $\mu\text{m}$ . The image (b) shows particle size of 3.5  $\mu\text{m}$ . The image (b) shows particle size of 4.1  $\mu\text{m}$ . The image (b) shows particle size of 5.3  $\mu\text{m}$ . For all the samples, the particle sizes vary between 3 - 6  $\mu\text{m}$ .

is difficult to do so using XRD analysis techniques, because of the close atomic numbers of boron and carbon (48). Chemical analysis has been used extensively in literature to find out the carbon concentration in boron carbides (49; 50). However, chemical analysis can overestimate the carbon present in the samples due to the presence of free carbon in boron carbides. In the present work, we have deduced the approximate carbon content of the boron carbides synthesized through their lattice parameters (8; 50). In the literature, the carbon concentration was deduced as a function of three parameters - the hexagonal cell parameters  $a$  and  $c$  and the rhombohedral cell volume  $V$ . The lattice parameters for the syntheses were determined by the Le Bail refinement using the software Powdercell (51). The unit cell volume values were then compared with the reference values in the literature (8; 50) and an estimate of the carbon content was deduced (table 3). These analyses were done for the boron carbides synthesised from amorphous carbon at the temperatures where boron carbide first appears.

Results show that the carbon content in boron carbides decreases with increase of the pressure of synthesis. This can be attributed to the lower diffusion of carbon in boron as the pressure increases, leading to the incorporation of a smaller amount of carbon in the unit cells: this argument also holds true for the rise of formation temperature with increase in pressure, for the same reasons as given above *i.e.* temperature acts as negative pressure.

Thus, we propose pressure as a way to modify the carbon concentration of boron carbides.

P (GPa)	T (K)	Reactants	$a$ (Å)	$c$ (Å)	$V$ (Å <sup>3</sup> )	at. % C
5	2473	$\beta$ B + graphite	5.617	12.160	332.251	12.8 - 16
5	2273	$\beta$ B + amorph. C	5.634	12.125	333.41	12.8 - 16
5	1873	amorph. B + amorph. C	5.628	12.091	331.69	12.8 - 16
2	2273	$\beta$ B + graphite	5.613	12.091	329.941	16 - 17.4
2	2073	$\beta$ B + amorph. C	5.600	12.114	329.095	17.4 - 18.7
2	1873	amorph. B + amorph. C	5.596	12.079	327.628	>18.7

Table 3: Atomic carbon concentration of the synthesised boron carbides recovered and characterised at ambient conditions as a function of the hexagonal cell parameters ( $a$  and  $c$ ) and the rhombohedral cell value ( $V$ ) in ascending order of carbon concentration. The reference values for determining the carbon concentration from the cell volume were taken from Ref. (50) and (8).

#### 4.4. Effect of thermal cycling versus constant temperature increase

During the *in situ* experiment at 13 GPa, it was found that boron carbide formed in the last cycle when the temperature was raised to 2433 K when temperature was increased through thermal cycling. When the same experiment was repeated without the thermal cycling in *ex situ* conditions at 2473 K, no boron carbide was formed. In both cases, the measured pressure was identical (within 0.5 GPa). This established that the formation temperature of boron carbide from elements at 13 GPa is above 2473 K, when steady heating is used. Hence, it is evident that the thermal cycling had played a role in the synthesis of boron carbide from its elements at a lower temperature.

Some work has been done in the literature on the effects of thermal cycling in chemical reactions. Barratt *et al.* (28) have shown through computational models that some hypothetical processes generate higher yields under forced thermal cycling than under single, fixed temperature conditions. Thermal cycling can also hasten phase transitions in some cases, as shown by Lee *et al.* (29). They have shown the kinetic transition of  $\gamma$  Fe-17 wt % Mn alloy into  $\epsilon$  phase due to thermal cycling: this can be attributed to the increase in transformation kinetics at the numerous nucleation sites introduced through thermal cycling.

Luk'yanenko *et al.* (30) have performed both theoretical and experimental investigations into the effect of thermal cycling on the high temperature interaction of titanium with gases like oxygen and nitrogen. They report that thermal cycling had intensified the diffusion displacements of impurity atoms. The diffusion coefficients of these oxygen and nitrogen impurity atoms increase both in the matrix and in the newly-formed phase. This had strongly affected the conditions of formation and growth of the new phase because the number of possible nucleation centers on the phase boundary had permanently increased with time and the energy barrier of the phase transformation has decreased as well.

Thus, we find that the dilation/densification cycles applied to  $\beta$  boron structure favours the diffusion of carbon atoms, leading to nucleation sites of boron carbide. This has resulted in the formation of boron carbide at a lower temperature than that would be needed by a steady fixed temperature condition.

In this case, we exclude the possibility of formation of a eutectic boron carbide - carbon mixture synthesised from melt, as has been observed in

(52; 53). This is because we found no evidence of melting in the EDXRD spectra obtained at each heating cycle.

## 5. Conclusions

In the present work, we have synthesised boron carbide at 2 GPa, 5 GPa and 13 GPa. The optimum synthesis parameters of boron carbide at pressures up to 5 GPa from its elements (boron and carbon) have been studied using the large volume Paris-Edinburgh press. It is established that the formation temperature of boron carbide strongly depends on pressure.

Amorphous boron is shown to be a better reactant than  $\beta$  boron for the synthesis of boron carbide, since it reduces the formation temperature at 2 GPa and at 5 GPa. This is similar to the trend observed before where amorphous carbon results in lower temperature of formation of boron carbide both at 2 GPa and 5 GPa, when compared with graphite.

Moreover, the mechanism of formation of boron carbide is also found to be dependent on pressure. An intermediate phase of  $\alpha$  boron has been observed before the formation of boron carbide at 5 GPa. This intermediate phase is absent during syntheses below 2 GPa and above 13 GPa.

We have found that the carbon concentration of boron carbide depends on the pressure value at which it is synthesised, and thus, we propose pressure as a means to control carbon concentration in boron carbides.

The synthesis experiments at the higher pressure value of 13 GPa have been performed for the first time. We have shown that the formation temperature of boron carbide from  $\beta$  boron and amorphous carbon is at least above 2473 K, with steady heating. The temperature of synthesis of boron carbide has been shown to decrease with thermal cycling that allows easier diffusion of carbon into the boron structure. Thus, thermal cycling can be investigated as a tool in bringing down the formation temperature in other chemical reactions as well.

## Acknowledgements

Supports from the DGA (France) and from the program NEEDS-Matériaux (France) are gratefully acknowledged. The authors thank Benoit Baptiste, Keevin Béneut, Ludovic Delbes, Antoine Jay, Hicham Moutaabbid, Silvia Pandolfi and Aminata Doucouré for useful discussions. The X-ray diffraction platform and the Raman spectroscopy platform in IMPMC is also acknowledged. The PhD fellowship for A. Chakraborti has been provided by

the Ecole Doctorale of Institut Polytechnique de Paris. We acknowledge SOLEIL for the provision of synchrotron radiation facilities.

## References

- [1] I. Caretti, R. Gago, J. M. Albella, and I. Jimenez, “Boron carbides formed by coevaporation of B and C atoms: Vapor reactivity,  $B_xC_{1-x}$  composition, and bonding structure,” *Physical Review B*, vol. 77, p. 174109, 2008.
- [2] M. Herrmann, I. Sigalas, M. Thiele, M. Müller, H.-J. Kleebe, and A. Michaelis, “Boron suboxide ultrahard materials,” *International Journal of Refractory Metals and Hard Materials*, vol. 39, pp. 53 – 60, 2013.
- [3] T. Roy, C. Subramanian, and A. Suri, “Pressureless sintering of boron carbide,” *Ceramics International*, vol. 32, pp. 227 – 233, 2006.
- [4] M. Kakiage, Y. Tominaga, I. Yanase, and H. Kobayashi, “Synthesis of boron carbide powder in relation to composition and structural homogeneity of precursor using condensed boric acid–polyol product,” *Powder Technology*, vol. 221, pp. 257 – 263, 2012.
- [5] F. Thévenot, “Boron carbide—a comprehensive review,” *Journal of the European Ceramic Society*, vol. 6, pp. 205–225, 1990.
- [6] A. K. Suri, C. Subramanian, J. K. Sonber, and T. S. R. C. Murthy, “Synthesis and consolidation of boron carbide: a review,” *International Materials Reviews*, vol. 55, pp. 4–40, 2010.
- [7] A. Alizadeh, E. Taheri-Nassaj, N. Ehsani, and H. R. Baharvandi, “Production of boron carbide powder by carbothermic reduction from boron oxide and petroleum coke or carbon active,” *Advances in Applied Ceramics*, vol. 105, pp. 291–296, 2006.
- [8] D. Gosset, *Properties of  $B_4C$* , 2nd ed., R. Konings and R. Stolle, Eds. Elsevier, 2020.
- [9] X. Q. Yan, Z. Tang, L. Zhang, J. J. Guo, C. Q. Jin, Y. Zhang, T. Goto, J. W. McCauley, and M. W. Chen, “Depressurization amorphization of single-crystal boron carbide,” *Physical Review Letters*, vol. 102, pp. 075 505–, 2009.

- [10] T. Fujii, Y. Mori, H. Hyodo, and K. Kimura, “X-ray diffraction study of  $B_4C$  under high pressure,” *Journal of Physics: Conference Series*, vol. 215, 2010.
- [11] V. A. Mukhanov, P. S. Sokolov, and V. L. Solozhenko, “On melting of  $B_4C$  boron carbide under pressure,” *Journal of Superhard Materials*, vol. 34, pp. 211–213, 2012.
- [12] P. Dera, M. H. Manghnani, A. Hushur, Y. Hu, and S. Tkachev, “New insights into the enigma of boron carbide inverse molecular behavior,” *Journal of Solid State Chemistry*, vol. 215, pp. 85–93, 2014.
- [13] A. Hushur, M. H. Manghnani, H. Werheit, P. Dera, and Q. Williams, “High-pressure phase transition makes  $B_{4.3}C$  boron carbide a wide-gap semiconductor,” *Journal of Physics: Condensed Matter*, vol. 28, p. 045403, 2016.
- [14] S. Mondal, E. Bykova, S. Dey, S. I. Ali, N. Dubrovinskaia, L. Dubrovinsky, G. Parakhonskiy, and S. van Smaalen, “Disorder and defects are not intrinsic to boron carbide,” *Scientific Reports*, vol. 6, p. 19330, 2016.
- [15] S. Chen, D. Z. Wang, J. Y. Huang, and Z. F. Ren, “Synthesis and characterization of boron carbide nanoparticles,” *Applied Physics A*, vol. 79, pp. 1757–1759, 2004.
- [16] B. Li-Hong, L. Chen, T. Yuan, T. Ji-Fa, H. Chao, W. Xing-Jun, S. Cheng-Min, and G. Hong-Jun, “Single crystalline boron carbide nanobelts: synthesis and characterization,” *Chinese Physics B*, vol. 17, pp. 4247–4252, 2008.
- [17] A. Jay, O. Hardouin Duparc, J. Sjakste, and N. Vast, “Theoretical phase diagram of boron carbide from ambient to high pressure and temperature,” *Journal of Applied Physics*, vol. 125, p. 185902, 2019.
- [18] A. Jay, “In silico design of a new phase of boron carbide,” Ph.D. dissertation, École Polytechnique, Palaiseau, 2014.
- [19] E. A. Ekimov, V. A. Sidorov, N. N. Mel’nik, S. Gierlotka, and A. Presz, “Synthesis of polycrystalline diamond in the boron carbide–graphite and boron–graphite systems under high pressure and temperature,” *Journal of Materials Science*, vol. 39, pp. 4957–4960, 2004.

- [20] V. A. Sidorov and E. A. Ekimov, "Superconductivity in diamond," *Diamond and Related Materials*, vol. 19, pp. 351–357, 2010.
- [21] A. Chakraborti, N. Vast, and Y. Le Godec, "Synthesis of boron carbide from its elements at high pressures and high temperatures," *Solid State Sciences*, vol. 104, p. 106265, 2020.
- [22] U. Anselmi-Tamburini, Z. A. Munir, Y. Kodaera, T. Imai, and M. Ohyanagi, "Influence of synthesis temperature on the defect structure of boron carbide: Experimental and modeling studies," *Journal of the American Ceramic Society*, vol. 88, pp. 1382–1387, 2005.
- [23] Y. Wang, T. Uchida, R. Von Dreele, M. L. Rivers, N. Nishiyama, K.-i. Funakoshi, A. Nozawa, and H. Kaneko, "A new technique for angle-dispersive powder diffraction using an energy-dispersive setup and synchrotron radiation," *Journal of Applied Crystallography*, vol. 37, pp. 947–956, 2004.
- [24] R. C. Liebermann, "Multi-anvil, high pressure apparatus: a half-century of development and progress," *High Pressure Research*, vol. 31, pp. 493–532, 2011.
- [25] H. Huppertz, "Multianvil high-pressure / high-temperature synthesis in solid state chemistry," *Zeitschrift für Kristallographie - Crystalline Materials*, vol. 219, pp. 330–338, 2004.
- [26] A. Dewaele, G. Fiquet, D. Andrault, and D. Hausermann, "P-V-T equation of state of periclase from synchrotron radiation measurements," *Journal of Geophysical Research: Solid Earth*, vol. 105, pp. 2869–2877, 2000.
- [27] Y. Tange, Y. Nishihara, and T. Tsuchiya, "Unified analyses for P-V-T equation of state of MgO: A solution for pressure-scale problems in high P-T experiments," *Journal of Geophysical Research: Solid Earth*, vol. 114, 2009.
- [28] C. Barratt, D. Lepore, M. Cherubini, and P. Schwartz, "Computational Models of Thermal Cycling in Chemical Systems , 2: 19-27," *International Journal of Chemistry*, vol. 2, pp. 19–27, 2010.

- [29] Y.-K. Lee and C.-S. Choi, "Effects of thermal cycling on the kinetics of the  $\gamma \rightarrow \epsilon$  martensitic transformation in an Fe-17 wt pct Mn alloy," *Metallurgical and Materials Transactions A*, vol. 31, pp. 2735–2738, 2000.
- [30] O. H. Luk'yanenko, V. S. Pavlyna, A. T. Pichugin, and V. M. Fedirko, "Effect of thermal cycling on high-temperature interaction of titanium with gases," *Materials Science*, vol. 33, pp. 739–750, 1997.
- [31] K. Cherednichenko, "Boron chalcogenides under extreme conditions," Ph.D. dissertation, Universite Pierre et Marie Curie - Paris VI, 2015.
- [32] H. Clark and J. Hoard, "The crystal structure of boron carbide," *Journal of the American Chemical Society*, vol. 65, pp. 2115–2119, 1943.
- [33] C. B. Wang, S. Zhang, Q. Shen, and L. M. Zhang, "Investigation on reactive sintering process of boron carbide ceramics by xrd," *Materials Science and Technology*, vol. 25, pp. 809–812, 2009.
- [34] S. Roszeitis, B. Feng, H.-P. Martin, and A. Michaelis, "Reactive sintering process and thermoelectric properties of boron rich boron carbides," *Journal of the European Ceramic Society*, vol. 34, pp. 327–336, 2014.
- [35] G. Parakhonskiy, N. Dubrovinskaia, E. Bykova, R. Wirth, and L. Dubrovinsky, "Experimental pressure-temperature phase diagram of boron: resolving the long-standing enigma," *Scientific reports*, vol. 1, pp. 96–96, 2011.
- [36] W. Yang, G. Shen, Y. Wang, and H.-k. Mao, "A scanning angle energy-dispersive x-ray diffraction technique for high-pressure structure studies in diamond anvil cells," *High Pressure Research*, vol. 28, pp. 193–201, 2008.
- [37] A. R. Oganov, J. Chen, C. Gatti, Y. Ma, Y. Ma, C. W. Glass, Z. Liu, T. Yu, O. O. Kurakevych, and V. L. Solozhenko, "Ionic high-pressure form of elemental boron," *Nature*, vol. 457, pp. 863–867, 2009.
- [38] B. Callmer, "An accurate refinement of the beta-rhombohedral boron structure locality: synthetic," *Acta Crystallographica Section B*, vol. 33, pp. 1951–1954, 1977.

- [39] A. Kouchi, *Amorphous Carbon*. Springer Berlin Heidelberg, 2011, pp. 41–42.
- [40] M. A. Caro, A. Aarva, V. L. Deringer, G. Csányi, and T. Laurila, “Reactivity of amorphous carbon surfaces: Rationalizing the role of structural motifs in functionalization using machine learning,” *Chemistry of Materials*, vol. 30, pp. 7446–7455, 2018.
- [41] J. Robertson, “Amorphous carbon,” *Advances in Physics*, vol. 35, pp. 317–374, 1986.
- [42] S. Limandri, G. Garbarino, D. Sifre, M. Mezouar, and V. Galván Josa, “Pressure dependence of the silicon carbide synthesis temperature,” *Journal of Applied Physics*, vol. 125, p. 165902, 2019.
- [43] D. Portehault, G. Gouget, C. G. Stary, and C. Sanchez, “Nanostructured amorphous boron material,” Patent WO2016207558A1, 2016.
- [44] W. Yang, W. Ao, J. Zhou, J. Liu, K. Cen, and Y. Wang, “Impacts of particle size and pressure on reactivity of boron oxidation,” *Journal of Propulsion and Power*, vol. 29, pp. 1207–1213, 2013.
- [45] S. Shalamberidze, G. Kalandadze, K. D.E., and B. Tsursumia, “Production of alpha rhombohedral boron by amorphous boron crystallization,” *Solid State Chemistry*, vol. 154, pp. 199–203, 2000.
- [46] H.-H. Carstensen, A. M. Dean, and R. W. Carr, *Chapter 4 The Kinetics of Pressure-Dependent Reactions*. Elsevier, 2007, vol. 42, pp. 101–184.
- [47] A. L. Patterson, “The Scherrer Formula for X-Ray Particle Size Determination,” *Physical Review*, vol. 56, pp. 978–982, 1939.
- [48] D. Gosset and M. Colin, “Boron carbides of various compositions: An improved method for x-rays characterisation,” *Journal of Nuclear Materials*, vol. 183, 1991.
- [49] K. A. Schwetz and P. Karduck, “Investigations in the boron-carbon system with the aid of electron probe microanalysis,” *Journal of the Less Common Metals*, vol. 175, pp. 1–11, 1991.
- [50] T. L. Aselage and R. G. Tissot, “Lattice constants of boron carbides,” *Journal of the American Ceramic Society*, vol. 75, pp. 2207–2212, 1992.

- [51] W. Kraus and G. Nolze, “*POWDER CELL* - a program for the representation and manipulation of crystal structures and calculation of the resulting X-ray powder patterns,” *Journal of Applied Crystallography*, vol. 29, pp. 301–303, 1996.
- [52] E. A. Ekimov, V. Ralchenko, and A. Popovich, “Synthesis of superconducting boron-doped diamond compacts with high elastic moduli and thermal stability,” *Diamond and Related Materials*, vol. 50, pp. 15–19, 2014.
- [53] E. A. Ekimov, V. P. Sirotinkin, T. B. Shatalova, and S. G. Lyapin, “Thermally stable, electrically conductive diamond material prepared by high-pressure, high-temperature processing of a graphite + boron carbide mixture,” *Inorganic Materials*, vol. 51, pp. 225–229, 2015.